

# Chapter 5

## *In vitro* modelling of the human blood-brain barrier

### Contents

<b>5.1 – INTRODUCTION.</b> ....	261
<b>5.2 – SPECIFIC AIMS.</b> ....	266
<b>5.3 – RESULTS.</b> .....	267
5.3.1 – Monolayer integrity evaluation using TEER.....	267
5.3.2 – Monolayer integrity evaluation using Na-Flu. ....	267
5.3.3 - Expression of tight junction proteins in hCMEC/D3 cells.....	268
5.3.4 - Transfection of hCMEC/D3 cells. ....	270
5.3.5 - Design and synthesis of hBCAT lentiviral plasmids. ....	278
5.3.5.1 - Synthesis of hBCAT shRNA plasmids. ....	280
<b>5.4 – DISCUSSION.</b> ....	285
5.4.1 – Validation of hCMEC/D3 monolayers as a representation of the BBB.....	285
5.4.2 – Transfection of the hCMEC/D3 cell line. ....	286
5.4.3 – Development of lentiviral vectors for stable inducible transfection.....	287
5.4.4 – Summary. ....	289

## **5.1 – INTRODUCTION.**

Until recently, it was assumed that the cellular distribution of the hBCAT proteins in the human brain would be the same as that observed in earlier rat brain studies; whereby BCATc is localised to the neuronal cells, and BCATm to the astrocytes (Sweatt *et al.* 2004; Garcia-Espinosa *et al.* 2007, Cole *et al.*, 2012). However, a study found that hBCATm is absent from astrocytes and instead detected in the endothelial cells of the brain vasculature (Hull *et al.*, 2012). A follow up investigation later found that hBCATm expression was significantly increased in the brains of patients with AD (Hull *et al.*, 2015). The implications of this unique expression of hBCATm are not completely understood and thus models of brain microvasculature were developed in this thesis to support further investigation.

In previous experiments, animal endothelial cells were used for vascular models (Audus & Borchardt, 1986), however, due to the unique expression of hBCATm in the human cerebrovasculature (Hull *et al.*, 2012) a different model was required. The hCMEC/D3 human endothelial cell line was developed and first described by Weksler *et al.* (2005) and is currently a widely used component of human BBB *in vitro* models (Vu *et al.*, 2009; Förster *et al.*, 2008; Poller *et al.*, 2008). The cell line is derived from primary human cells and optimised with the aim of maintaining the characteristics of primary cultures, but with less demanding culture conditions (Weksler *et al.*, 2005). It has been well characterised and is known to express many of the vital tight junction proteins unique to human brain microvasculature (Weksler *et al.*, 2005, 2013; Poller *et al.*, 2003). A co-culture of hCMEC/D3 cells with either primary human astrocytes, or with the SH-SY5Y neuronal cell line has previously been described, although not of the three cell lines together (**Figure 5.1**) (Hatherell *et al.*, 2011; Freese *et al.*, 2014). Activity of hBCAT in a tri-culture system could be controlled using selective hBCAT isoform inhibitors, RNAi, or overexpression plasmid transfection. The purpose of developing this model would be twofold.

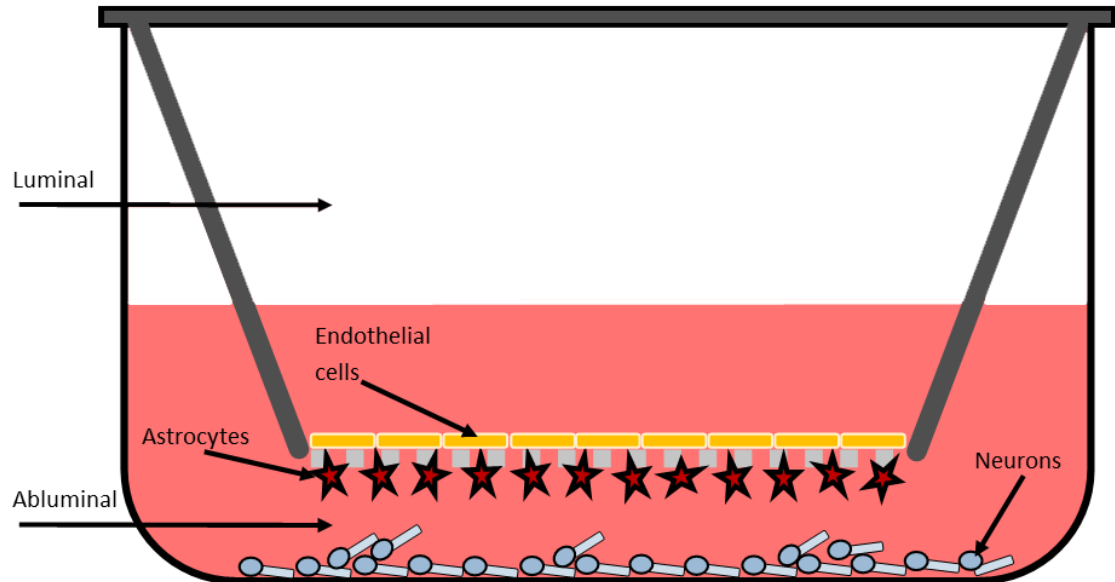


**Figure 5.1** – Representation of a culture well insert and the contributing cells. An *in vitro* model of the BBB can be constructed by growing astrocytes and neurons abluminal to an endothelial monolayer. This could be utilised to investigate cell-cell interactions and the transport or metabolism of nutrients through the monolayer.

Firstly, to observe metabolic changes to the BCAAs and L-glutamate as the compounds pass from the luminal (circulation) to the abluminal (brain compartment). Such studies would be able to ascertain if dysregulated expression of hBCATm has an influence on brain concentration of nutrients such as the BCAAs, L-glutamate, L-glutamine, and keto acids. It was originally hypothesised by Hull *et al.*, (2015) that increased hBCAT expression may contribute toward an excitotoxic concentration of L-glutamate as well as a potential toxic accumulation of keto acids.

Secondly, to study the effect of hBCATm on BBB integrity. Maintenance of the barrier is essential to prevent migration of xenobiotic compounds, endogenous immune cells, A $\beta$ , and also to protect the brain from fluctuations in blood nutrients (Togo *et al.*, 2002; Zlokovic, 2011). This could be investigated by modifying the expression of hBCAT in the co-culture, before using transendothelial electrical resistance (TEER) and fluorescent compound transmission studies to assess permeability, or western blot analysis to confirm tight junction protein expression (Eigenmann *et al.*, 2013). Identification of hBCAT expression as a modulator of BBB integrity could provide a future target for treatment.

The third and final aim of this thesis is therefore to develop a model of the human cerebrovasculature, to investigate the impact of endothelial hBCATm on amino acid metabolism, and to investigate the effect of hBCATm expression on BBB integrity.

In this study hCMEC/D3 cells were cultured on collagen-coated inserts and integrity of the resultant barrier evaluated by measuring transepithelial resistance (TEER) as well as sodium fluorescein (Na-Flu) diffusion. Western blot analysis confirmed the expression of VE-cadherin, occludin, and ZO-1, which are involved in the formation of adhesion and tight junctions (Weksler *et al.*, 2005, 2013). Finally, several experiments sought to optimise the transfection of hCMEC/D3 cells using a range of different conditions. Although the cells proved to be resistant to transfection, lentiviral transduction is described as effective in transducing hCMEC/D3 cells (Mizee *et al.*, 2013), and thus new

plasmids were developed for future synthesis of lentiviral particles. The lentiviral plasmid chosen contains a gene for the TetR repressor which is constitutively expressed in transduced cells (**Figure 5.2**). This binds to the promotion site and prevents transcription of the desired downstream gene or shRNA. However, in treated cells, tetracycline or doxycycline will bind the TetR repressor molecule and sterically hinder repressor binding to the Tet promotion region. This then allows transcription of the target downstream of the Tet promoter (Wiederschain *et al.*, 2009) (**Figure 5.2**).

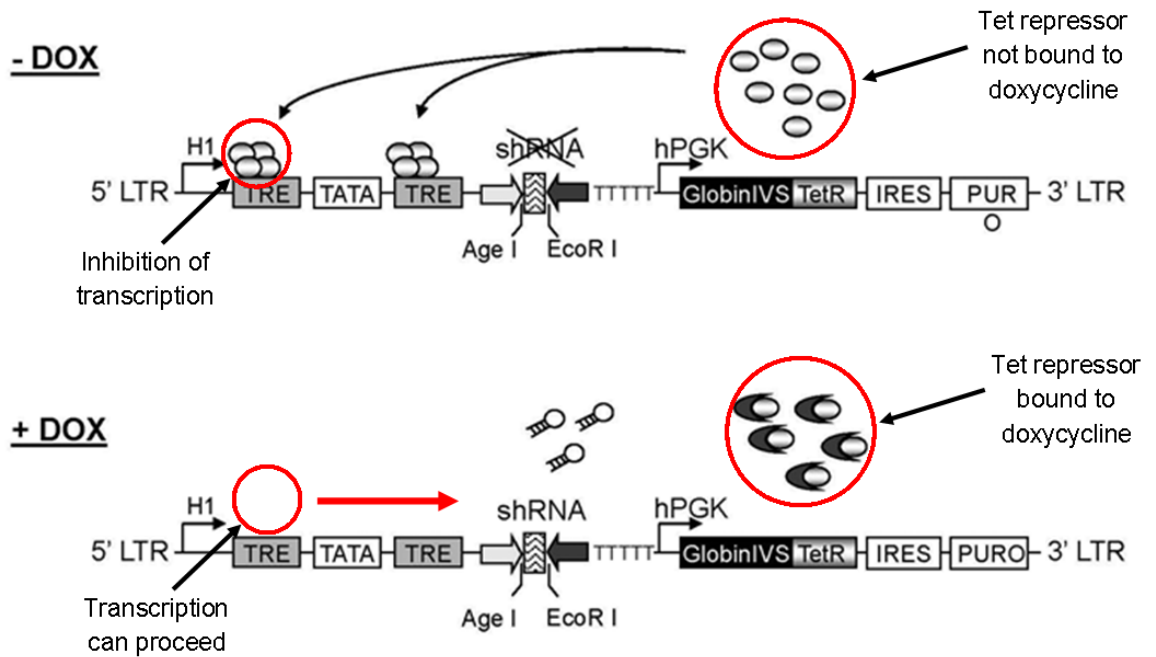


**Figure 5.2 – Tetracycline inducible transcription of shRNA.** The TetR repressor protein is constitutively expressed (promoted by hPGK) and binds to the tetracycline responsive element (TRE) to inhibit translation of shRNA. This process is inhibited by cell treatment with tetracycline or doxycycline (DOX) which interacts with TetR and causes a conformational change preventing inhibitory binding to the TRE. Adapted from Wiederschain *et al.* (2009).

## **5.2 – SPECIFIC AIMS.**

1. Optimise conditions for a co-culture of hCMEC/D3, SH-SY5Y, and astrocytic cells as a model of the human BBB.
2. Validate the model of the human BBB using permeability studies and key protein expression studies.
3. Modify hBCAT expression in cells of the human BBB model.
4. Evaluate the impact of hBCAT dysregulation on cell metabolism and monolayer permeability.

## **5.3 – RESULTS.**

### **5.3.1 – Monolayer integrity evaluation using TEER.**

The EVOM Epithelial Volt/Ohm meter was used in combination with either a 6-well or 12-well EndOhm chamber to estimate insert resistance in  $\Omega \times$  surface area in  $\text{cm}^2$ . Monolayer resistance was measured both as a monoculture and as a co-culture with C6 rat glioma cells, and the resistance of a blank insert subtracted from each sample. A monolayer with a higher TEER value is considered less permeable than one with a lower value as a common indicator of a free flow of small electrolytes (Smith *et al.*, 2004; Weksler *et al.*, 2005). Previous work with the hCMEC/D3 cell line has found TEER values of monolayers as high as  $300 \Omega \times \text{cm}^2$  (Abbott *et al.*, 2012).

Measurement of TEER at all time points and well sizes showed a low resistance for all samples. Firstly, test inserts containing mono-cultured hCMEC/D3 barrier growth showed resistance only slightly higher than blank inserts. It was found that the 6-well test inserts had a resistance between  $4.67$  and  $9.34 \Omega \times \text{cm}^2$  (N=5) after subtraction of the blank, which was comparable to the 12-well test inserts ( $6.72 - 7.84 \Omega \times \text{cm}^2$ ; N=20). Furthermore, co-culture with C6 astrocytes had no impact on TEER value, which was found to be identical to that of the mono-culture for both 6-well (N=4) and 12-well (N=10) plate inserts.

### **5.3.2 – Monolayer integrity evaluation using Na-Flu.**

The integrity of a hCMEC/D3 monolayer was measured by assaying the diffusion of fluorescent dye through the membrane, from the apical to basal chamber, and the results used to validate the BBB model. The diffusion of dye through a blank insert was subtracted from that of seeded test inserts and permeability expressed as  $P_e$  ( $\times 10^{-3} \text{ M cm min}^{-1}$ ). Previous work found the  $P_e$  of hCMEC/D3 monolayers to be between  $3.4$  and  $5.5 \times 10^{-3} \text{ M cm min}^{-1}$  (Förster *et al.*, 2008). A lower  $P_e$  value is considered to indicate a less permeable membrane than a higher value.

The permeability of monolayers cultured on both sizes of insert was found to vary over time. Here, it was found that  $P_e$  ranged between 4.84 and 13.44  $\times 10^{-3}$  M cm  $\text{min}^{-1}$  for 6-well inserts, and between 9.57 and 18.93  $\times 10^{-3}$  M cm  $\text{min}^{-1}$  for 12-well inserts (**Figure 5.3**). Inserts were first assayed three days after hCMEC/D3 cell seeding, and recorded for both insert size as approximately 10  $\times 10^{-3}$  M cm  $\text{min}^{-1}$ . In both cases, permeability gradually increased until day six, and then gradually decreased (**Figure 5.3**). Throughout the study, permeability of the 6-well inserts was lower than that of the 12-well inserts. In particular, on the last day of the study (day 18), the  $P_e$  value was recorded as 5.75  $\times 10^{-3}$  M cm  $\text{min}^{-1}$  and 14.54  $\times 10^{-3}$  M cm  $\text{min}^{-1}$  for the 6-well and 12-well inserts, respectively (**Figure 5.3**). It was determined that cultures grown on 6-well plate inserts were roughly the same as that seen in previous studies (Förster *et al.*, 2008) and would be acceptable for use as a model of BBB integrity. Monolayers formed on 12-well inserts were considerably more permeable although the reason for this is unknown. Co-cultures with astrocytes were not assayed with the Na-Flu assay in this thesis, but it is well documented that this can further decrease hCMEC/D3 monolayer permeability and this will be targeted in future work (Hatherall *et al.*, 2011; Weksler *et al.*, 2013; Freese *et al.*, 2014).

### 5.3.3 - Expression of tight junction proteins in hCMEC/D3 cells.

Restriction of movement through the BBB is dependent on the close adhesion of endothelial cells preventing the passive flow of many molecules, ions, or larger entities such as proteins and cells. These tight junctions are maintained by proteins such as VE-cadherin, occludin, and ZO-1, and western blot analysis confirming the expression of these proteins is required to further validate the model of human brain microvasculature. In this study, all three proteins were detected in hCMEC/D3 cells (Weksler *et al.*, 2005; Eigenmann *et al.*, 2013).

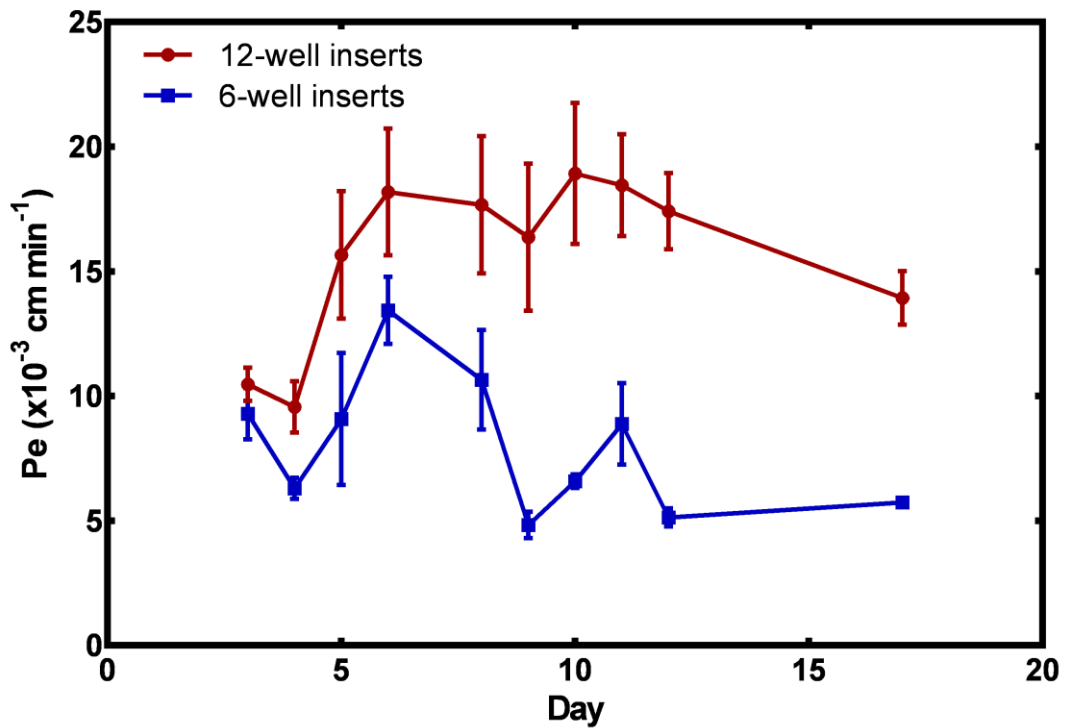


**Figure 5.3 — Permeability of hCMEC/D3 monolayers over time.** Cells were seeded on 6 or 12-well membrane inserts and cultured as previously described. The monolayer was assayed by measuring the amount of Na-Flu solution which passed from the apical to basal chamber. The permeability coefficient of a blank insert was subtracted from each value. Results are presented as means  $\pm$  standard error of the mean (6-well plate inserts N=5; 12-well plate inserts N=9).

First, two bands were observed upon probing for VE-cadherin, one band resolving at approximately 89 kDa and one at 115 kDa (**Figure 5.4; [A] [i]**). Previous studies have found that although the predicted molecular weight of VE-cadherin is 89 kDa, western blot analysis of the protein presents a band at 115 kDa due to glycosylation (Bach *et al.*, 1998; Geyer *et al.*, 1999). The expression of VE-cadherin can therefore be confirmed. Expression of occludin was confirmed by a single band at the expected molecular weight (**Figure 5.4; [A] [ii]**). Finally, a tight double band was observed on western blot analysis of ZO-1 protein at approximately 110 kDa (**Figure 5.4; [B] [i]**), however, the predicted MW for this protein is 230 kDa.

#### 5.3.4 - Transfection of hCMEC/D3 cells.

To assess the impact of hBCATm upregulation in AD brain there is a need to develop *in vitro* models of hBCATm expression. As previously described (**Chapter 4**), the SH-SY5Y cell line can be transfected with either hBCATm siRNA or hBCATm expression plasmid, validating the vectors. To expand this work, experiments aimed to optimise transfections of the hCMEC/D3 cell line, using the SH-SY5Y cell transfection method as a reference.

In the first instance, the hCMEC/D3 cell line was treated with either the hBCATm or hBCATc expression plasmids using the jetPRIME transfection reagent. Unfortunately, conditions which significantly increased expression of the respective isoform in SH-SY5Y cells (hBCATm: **Figure 4.9**. hBCATc: unpublished group data), did not affect expression in the hCMEC/D3 cells (**Figure 5.5; [A] [i] & [ii]**). Similarly, transfection of siRNA has been shown to effectively knock-down hBCATm expression in SH-SY5Y cells (**Figure 4.5**), but was not possible for hCMEC/D3 cells (**Figure 5.5; [A] [i] & [ii]**). Furthermore, relative standard curve qPCR demonstrated that 48 hours after transfection with a BCAT2 siRNA the mRNA copy number had not decreased and in fact appeared to have increased 100% (**Figure 5.5; [B] [i]**). As transfection of the hCMEC/D3 cell line was unsuccessful at this stage a range of different conditions were designed to establish an effective treatment.

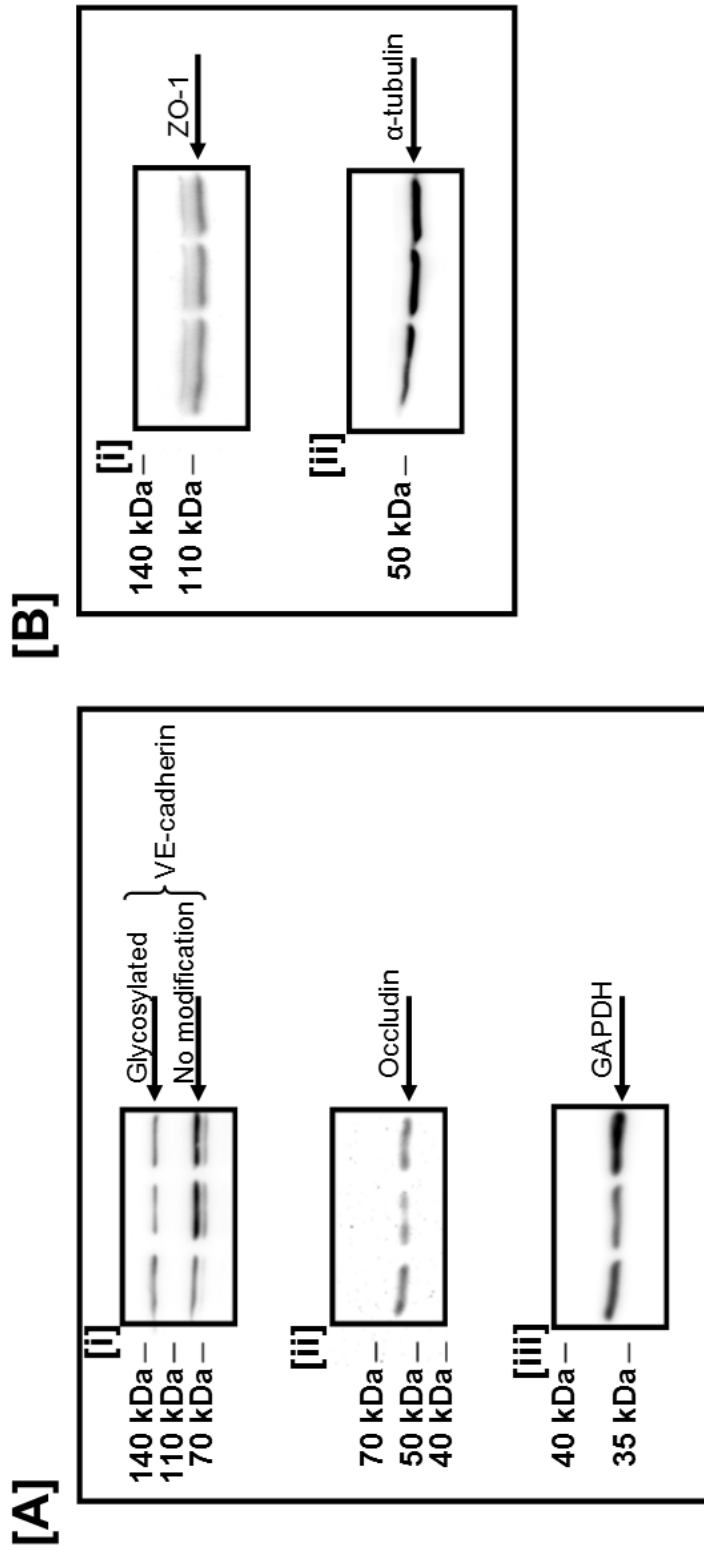


**Figure 5.4 — Expression of tight junction proteins in hCMEC/D3 cells.** Western blot analysis was performed on hCMEC/D3 cell lysate in triplicate for three proteins important to the function of vascular endothelial cells, particularly in the BBB. **[A]** Western blot analysis using antibodies against: **[i]** VE-cadherin (MW 89 kDa, or 115 kDa for glycosylated form), **[ii]** occludin (predicted MW 59 kDa), **[iii]** loading control GAPDH (predicted MW 35 kDa). **[B]** Western blot analysis using antibodies against: **[i]** ZO-1 (predicted MW 230 kDa), **[ii]** loading control  $\alpha$ -tubulin (predicted MW 50 kDa).

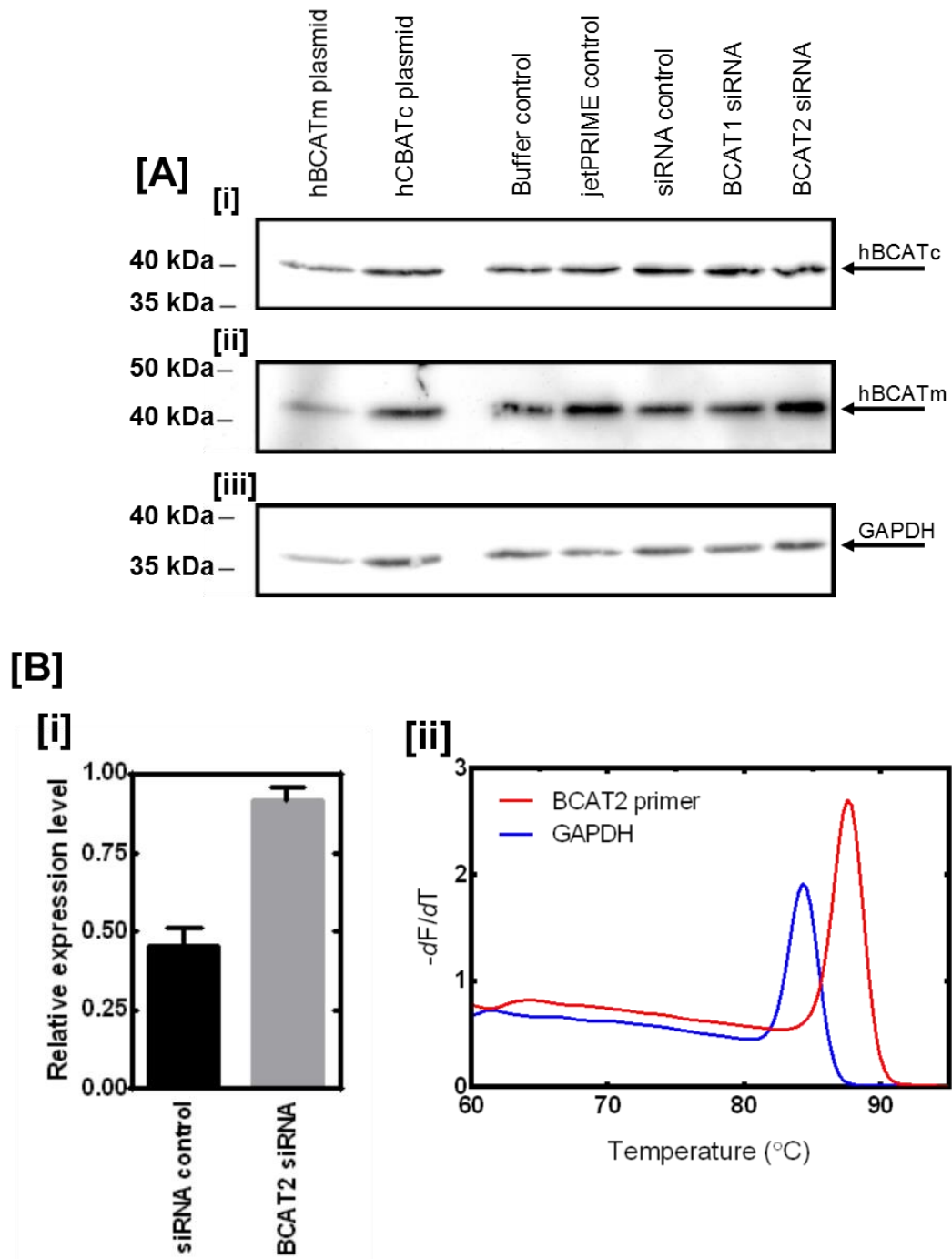


**Figure 5.5 — First transfections of hCMEC/D3 cells.** Using conditions optimised for SH-SY5Y cells, the hCMEC/D3 cell line was transfected with siRNA, plasmid, or control. A control with transfection buffer and reagent, but no nucleic acid was also used (jetPRIME control). **[A]** Western blot analysis of hCMEC/D3 cells: **[i]** hBCATc (predicted MW 41 kDa), **[ii]** hBCATm (predicted MW 43 kDa), **[iii]** GAPDH (predicted MW 35 kDa). **[B]** qPCR analysis of transfected hCMEC/D3 cells: **[i]** BCAT2 expression relative to GAPDH. The efficiency of GAPDH and BCAT2 primers was 97% and 98% respectively. **[ii]** Melt curve analysis of qPCR products. Predicted  $T_m$  using uMELT (Dwight *et al.*, 2011) for GAPDH product is 86.2 $^{\circ}\text{C}$ , and for BCAT2 product is 92.2 $^{\circ}\text{C}$ .

To optimise plasmid transfection, a range of different plasmids were trialed. First, cells were transfected with either 0.375 or 1.5  $\mu\text{g}$  eGFP plasmid, using a standard 1:2 ratio of plasmid  $\mu\text{g}$  to transfection reagent  $\mu\text{L}$ . The cells were imaged by fluorescence microscopy 48 hours post-transfection. It was observed that compared to the SH-SY5Y cells (**Figure 5.6; [A]**), transfection of hCMEC/D3 cells was poor when either 1.5  $\mu\text{g}$  (**Figure 5.6; [B]**) or 0.375  $\mu\text{g}$  (**Figure 5.6; [C]**) of plasmid was used. Next, time-point analysis was used to determine if there was any point at which overexpression could be observed. Cells were harvested 24, 48, 72, 96, and 120 hours post-transfection and analysed by western blot (**Figure 5.7**). However, no increase in hBCATm expression was observed at any time point.

Several different methods were also used for transfection of siRNA into hCMEC/D3 cells. Firstly, hCMEC/D3 cells were treated with a range of different concentrations of siRNA. However, western blot analysis of cells transfected with 12.5, 25, 50, and 100 nM BCAT2 siRNA using jetPRIME transfection reagent did not have an observable impact on hBCATm expression (**Figure 5.8**). Several studies have recently demonstrated successful siRNA transfection in hCMEC/D3 cells using the RNAiMAX transfection reagent (Le Guelte *et al.*, 2012; Artus *et al.*, 2014; Okura *et al.*, 2014). This reagent was therefore compared relative to jetPRIME for transfection efficiency of siRNA using a fluorescently labelled siRNA duplex. Using fluorescence microscopy, it was clearly observed that after 24 hours there was significant accumulation of fluorescent siRNA within SH-SY5Y cells using either transfection reagent (**Figure 5.9; [A]**). This fluorescence is spread throughout the cytoplasm of SH-SY5Y cells and focuses in what appears to be the nucleus of the SH-SY5Y cells. However, there was no significant cytoplasmic or nuclear fluorescence in hCMEC/D3 cells, rather, siRNA appeared to form extracellular punctate clumps (**Figure 5.9; [B]**) indicating transfection was inhibited. An identical cellular distribution was also observed when monitoring cells after 48 and 72 hours (data not shown).

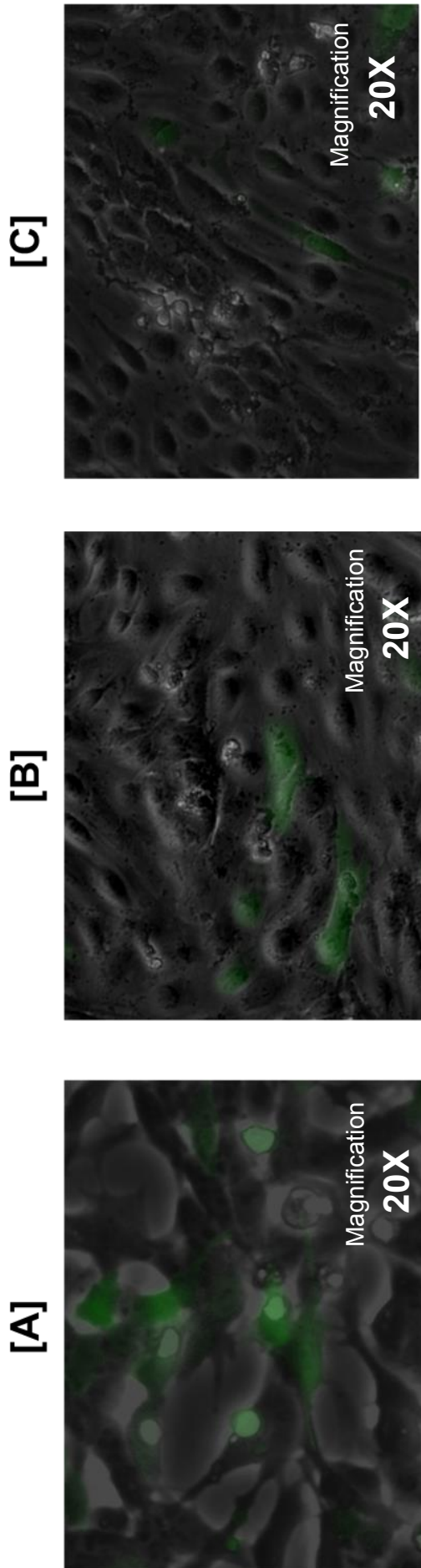


**Figure 5.6 — Transfection of eGFP plasmid in hCMEC/D3 and SH-SY5Y cells.** Cells were transfected using jetPRIME transfection reagent as previously described. Cells were imaged 48 hours post-transfection at 20X magnification, both with light microscopy and with fluorescence microscopy using an excitation/emission filter  $\lambda$  495/519 nm. A composite of these images was then produced which representatively displays the number of fluorescing cells. Cells were viewed under a Nikon Eclipse 50i microscope and images acquired with Simple PCI software and a QICAM colour 12-bit camera. **[A]** SH-SY5Y cells appear easily transfected and a high number of cells showing fluorescence were observed. **[B]** hCMEC/D3 cells transfected with 0.375  $\mu$ g plasmid and 0.75  $\mu$ L jetPRIME transfection reagent. **[C]** hCMEC/D3 cells transfected with 1.5  $\mu$ g eGFP plasmid and 3  $\mu$ L jetPRIME transfection reagent.

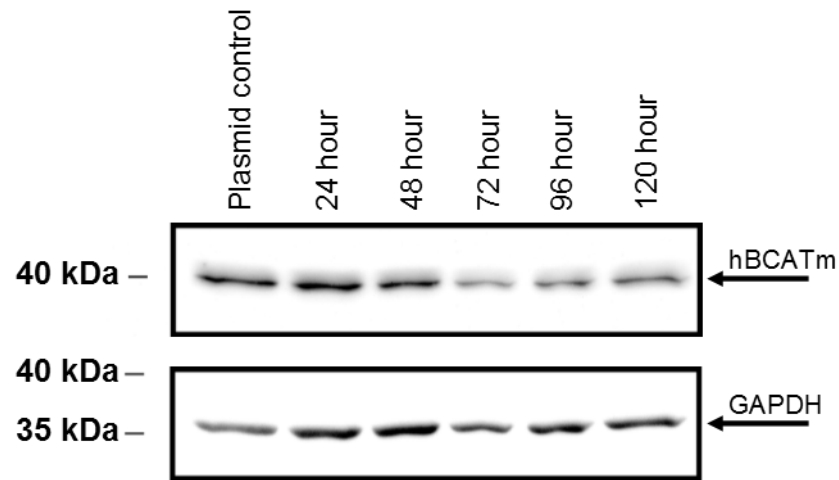


**Figure 5.7 — Timed hBCATm plasmid transfection.** Using conditions optimised by experiments with SH-SY5Y cells, the hCMEC/D3 cell line was transfected with hBCATm plasmid or eGFP plasmid control. Cells were harvested every 24 hours for 120 hours. Western blot analysis of hBCATm and GAPDH loading control (MW 43 kDa and 35 kDa, respectively) was used to determine the peak increase in hBCATm expression following transfection.

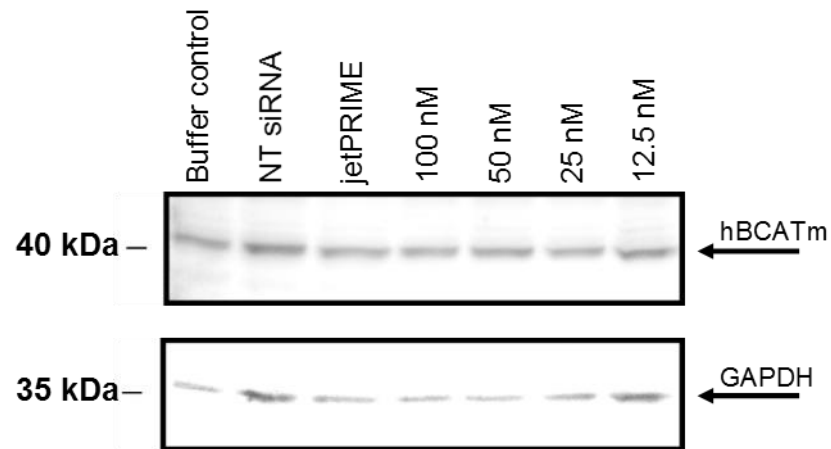


**Figure 5.8 — Titration of siRNA concentration with jetPRIME reagent.** hCMEC/D3 cells were transfected with either one of 4 different concentrations of an siRNA targeting BCAT2, a non-targeting siRNA control (siRNA control) or treated with a non-transfection control. Western blot analysis was used to determine the effect of the treatments on hBCATm expression.

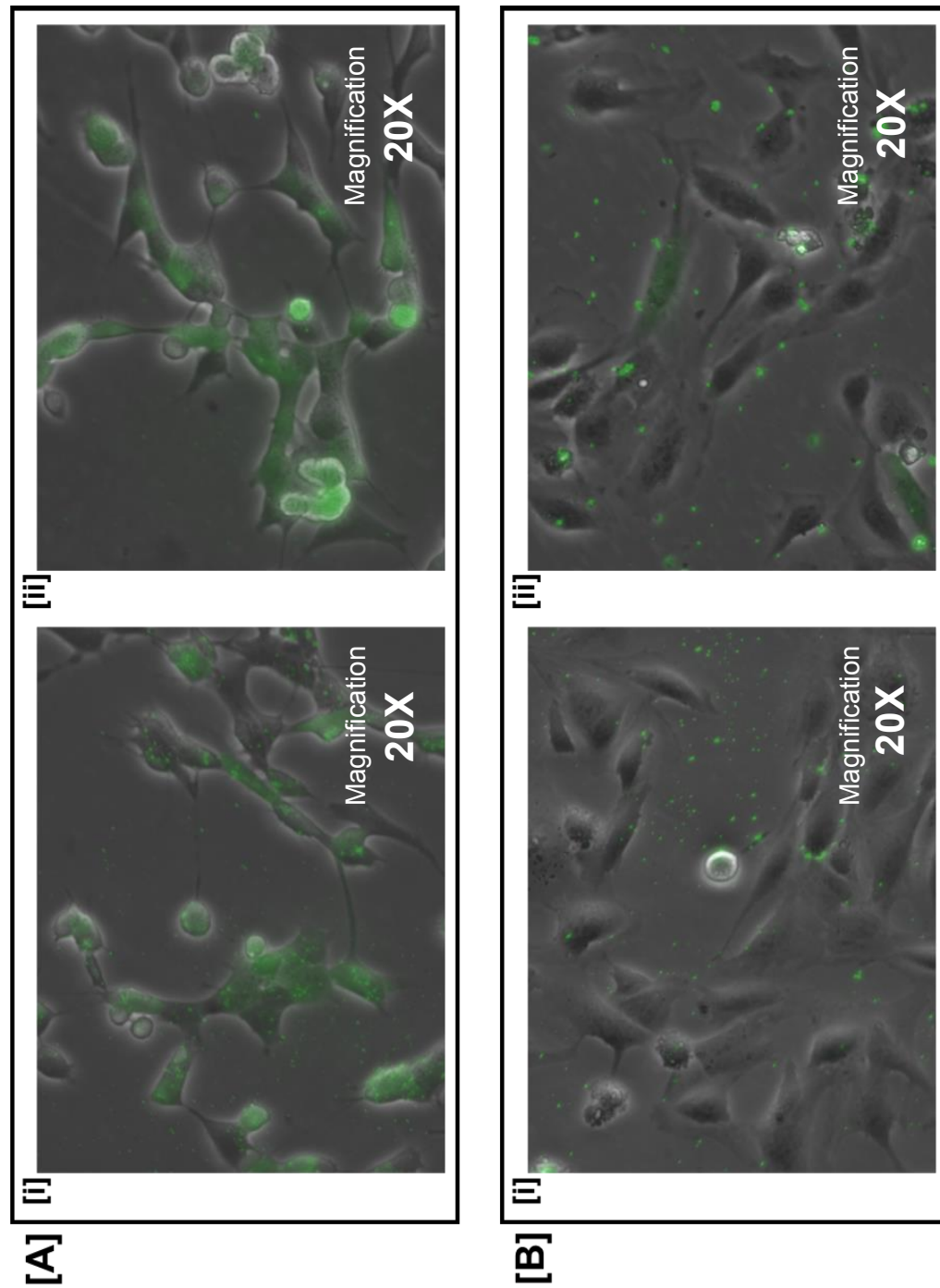


**Figure 5.9** — Transfection of cells with a fluorescently labelled siRNA. Cells were imaged 24 hours post-transfection at a 10X magnification with light and fluorescent microscopy using an excitation/emission filter  $\lambda$  495/519 nm. A composite of these images was then produced which representatively displays the number of fluorescing cells. Cells were viewed under a Nikon Eclipse 50i microscope and images acquired with Simple PCI software and a QICAM colour 12-bit camera. **[A]** SH-SY5Y cells transfected with **[i]** jetPRIME and **[ii]** RNAiMAX. **[B]** hCMEC/D3 cells transfected with **[i]** jetPRIME and **[ii]** RNAiMAX.

Finally, western blot analysis was utilised to compare knock-down of hBCATm in either SH-SY5Y or hCMEC/D3 cells (**Figure 5.10**). It was found that using RNAiMAX knock-down of hBCATm was effective in both cell lines, and more so in the hCMEC/D3 cells. Furthermore, in both cell lines, the treatment with the lowest concentration of siRNA had the greatest effect; specifically, 12.5 nM siRNA was able to decrease hBCATm expression 56% and 85% in SH-SY5Y and hCMEC/D3 cells, respectively.

In summary, plasmid transfection of SH-SY5Y cells has been demonstrated but proved unsuccessful for hCMEC/D3 cells under a range of conditions. To date there are no published studies of hCMEC/D3 plasmid transfection. Knock-down of hBCATm in hCMEC/D3 cells was demonstrated after optimisation, requiring a different method to that of SH-SY5Y transfection.

### **5.3.5 - Design and synthesis of hBCAT lentiviral plasmids.**

Lentiviral vectors were designed as viral transduction is reported as an effective method of genetic modification in hCMEC/D3 cells (Mizee *et al.*, 2013). The vectors will allow for the creation of stable cell lines which express the inserted sequence on treatment with tetracycline or a related compound. This would allow, for example, wild-type neurons and transduced endothelial cells to be treated with tetracycline and specifically induce hBCATm knock-down or overexpression in the endothelial cells. This avoids off-target effects of transfection in a co-culture, where the transfection mixture could affect several cell types in the co-culture.

In this study, separate plasmid backbones were developed for overexpression or knock-down. For short-hairpin RNA (shRNA) expression, the tet-pLKO.1-puro (pLKO) plasmid was used and the required shRNA inserted into the plasmid by ligation. Based on the validated siRNA sequence within this study, a BCAT2 shRNA sequence was designed and synthesised (pLKO-BCAT2). A similar plasmid containing a shRNA sequence for BCAT1 (pLKO-BCAT1) was provided and validated by another group (Tönjes *et al.*, 2013).

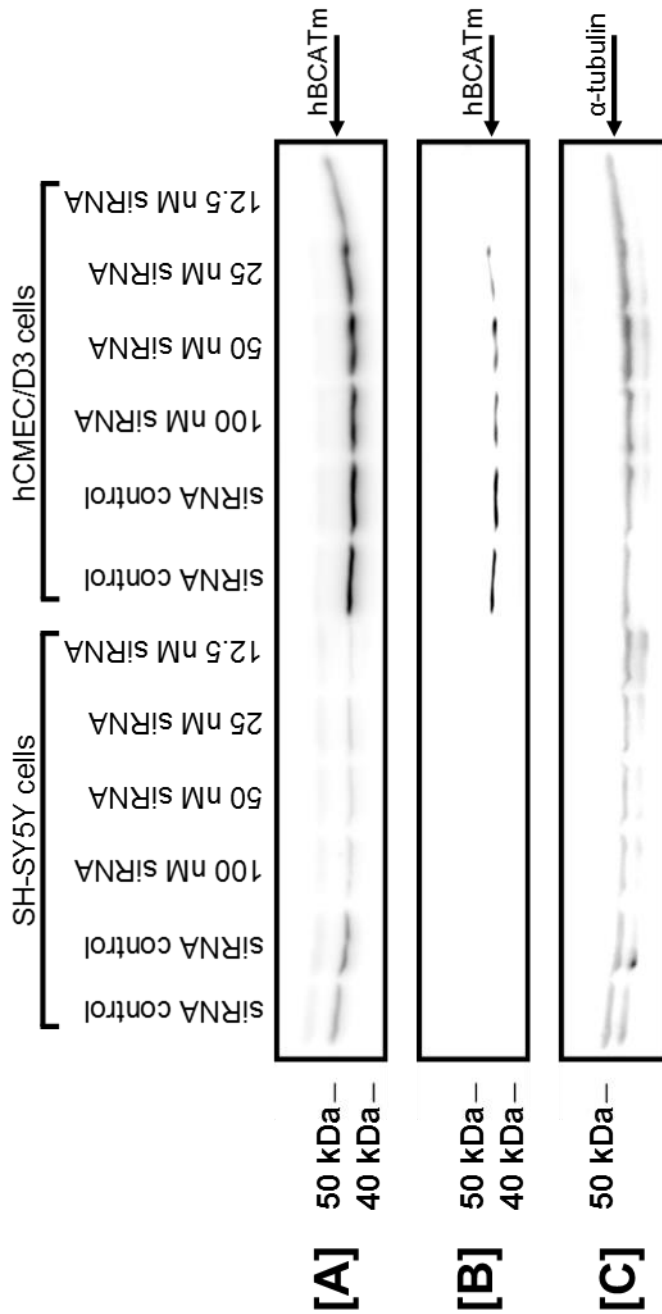


**Figure 5.10 — Knock-down of hBCATm in SH-SY5Y and hCMEC/D3 cells using RNAiMAX transfection reagent.** Cells were transfected with BCAT2 siRNA, or controls, and Western blot analysis used to compare the expression of hBCATm (predicted MW 43 kDa) in each sample. When normalised against  $\alpha$ -tubulin loading control predicted MW 50 kDa expression of hBCATm is lowest in both cell lines when 12.5 nM of siRNA is used. Expression of hBCATm is clearly higher in the hCMEC/D3 cell line. [A] A long exposure was required to show bands for SH-SY5Y hBCATm expression. [B] A shorter exposure of the same membrane clearly demonstrates the effect of siRNA in hCMEC/D3 cells. [C] Loading control.

For hBCAT overexpression, the pCW57.1 plasmid was used and the hBCATc (pCW57.1-BCAT1) or hBCATm (pCW57.1-BCAT2) gene cloned into the vector by homologous recombination, using BCAT gene donor plasmids supplied to order by an external manufacturer (Fisher Scientific, Loughborough). Synthesis was confirmed by partial sequencing of both plasmids using the pCEP-Forward primer (**Appendix B; 1 & 2**). It should be noted that the BCAT1 gene is cloned exactly as the cDNA sequence within the NCBI database, while the BCAT2 gene has been codon optimised for maximal expression in humans while retaining the same amino acid sequence (Kim *et al.*, 1997).

#### **5.3.5.1 - Synthesis of hBCAT shRNA plasmids.**

The pLKO-BCAT1 plasmid was kindly provided by Dr Bernhard Radlwimmer (Tonjes *et al.*, 2013) and was partially sequenced for confirmation using the H1 primer (**Appendix B; 3**). The pLKO-BCAT2 plasmid on the other hand, was synthesised in this study. First, a diagnostic digest was used to confirm purification of the pLKO plasmid (**Figure 5.11**). Using the previously validated BCAT2 siRNA sequences, an shRNA sequence was designed with an XhoI loop and complementary 4 base overhangs for AgeI and EcoRI (**Figure 5.12**), this was synthesised by an external laboratory (Eurofins MWG, Germany). The double stranded shRNA coding DNA insert was then ligated into the prepared linear plasmid. Sequencing of the plasmid using the H1 primer appeared to show a rapid termination midway through the BCAT2 shRNA sequence (**Figure 5.13**), possibly due to the XhoI hairpin loop, and as such only half of the shRNA could be sequenced. A diagnostic digest was recommended by the manufacturer (Wiederschain *et al.*, 2009), and confirmed ligation alongside the sequenced pLKO-BCAT1 plasmid as a control (**Figure 5.14**).

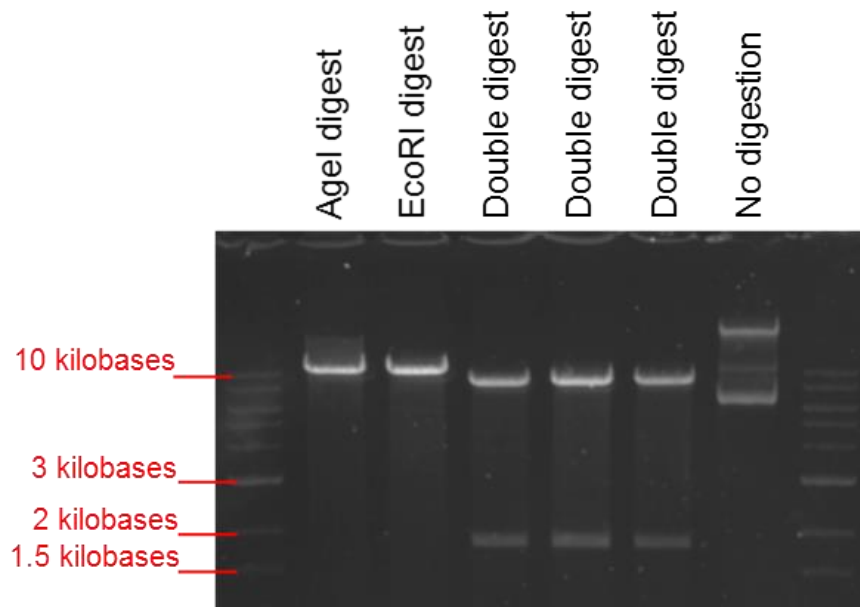


**Figure 5.11 — Digestion of pLKO plasmid.** The plasmid was digested using either the EcoRI or AgeI restriction enzymes as a single digest, or both as a double digest. Individual 0.8% agarose gel lanes were injected with either a digested plasmid solution, a mock digestion with no enzyme added, or 1 kb DNA ladder, and the gel electrophoresed. Once complete, the gel was stained with Diamond DNA stain and imaged using a UV transilluminator. It is instructed that a single digest with either restriction enzyme should produce a band resolving at 10.5 kilobases, while a double digested plasmid will produce two bands, resolving at 8.0 and 1.8 kilobases, respectively (Wiederschain *et al.*, 2009).

**BCAT2 cDNA sequence:**

ATGGCCGAGCCGCTCTGGGGCAGATCTGGGCACGAAAGCTTCTCTGTCCCTTGGCTTCTGTG  
 TGGTCCCAGAAGATATGCCTCCTCCAGTTTCAAGGCTGCAGACCTGCAGCTGGAAATGACACAGA  
 AGCCTCATAAGAAGCCTGGCCCCGGCGAGCCCCTGGTGTTTGGGAAGACATTTACCGACCACATG  
 CTGATGGTGGAAATGGAATGACAAGGGCTGGGGCCAGCCCCGAATCCAGCCCTTCCAGAACCTCAC  
 GCTGCACCCAGCCTCCTCCAGCCTCCACTACTCCCTGCAGCTGTTTGGAGGGCATGAAGGCGTTCA  
 AAGGCAAAGACCAGCAGGTGCGCCTCTTCCGCCCTGGCTCAACATGGACCGGATGCTGCGCTCA  
 GCCATGCGCCTGTGCCTGCCGAGTTTCGACAAGCTGGAGTTGCTGGAGTGCATCCGCCGGCTCAT  
 CGAAGTGGACAAGGACTGGGTCCCCGATGCCGCCGGCACCAGCCTCTATGTGCGGCCTGTGCTCA  
 TTGGGAACGAGCCCTCGCTGGGTGTCAGCCAGCCCACGCGCGCTCCTGTTTCGTCATTCTCTGC  
 CCAGTGGGTGCCCTACTTCCCTGGAGGCTCCGTGACCCCGGTCTCCCTCCTGGCCGACCCAGCCTT  
 CATCCGGGCCTGGGTGGGCGGGGTCGGCAACTACAAGTTAGGTGGGAATTATGGGCCACCGTGT  
 TAGTGCAACAGGAGGCACTCAAGCGGGCTGTGAACAGGT**CCTCTGGCTGTATGGGCCCGA**CCAC  
 CAGCTCACCGAGGTGGGAACCATGAACATCTTTGTCTACTGGACCCACGAAGATGGGGTGCTGGA  
 GCTGGTGACGCCCCGCTGAATGGTGTATCCTGCCTGGAGTGGTCAGACAGAGTCTACTGGACA  
 TGGCTCAGACCTGGGGTGAGTTCCGGGTGGTGGAGCGCACGATCACCATGAAGCAGTTGCTGCGG  
 GCCCTGGAGGAGGGCCGCTGCGGGAAGTCTTTGGCTCGGGCACCGCTTGCCAGGTCTGCCAGT  
 GCACCGAATCCTGTACAAAGACAGGAACCTCCACATCCCACCATGGAAAATGGGCCTGAGCTGA  
 TCCTCCGCTTCCAGAAGGAGCTGAAGGAGATCCAGTACGGAATCAGAGCCCACGAGTGGATGTTCC  
 CCGGTGTGA

**Oligonucleotide insert:**

**Figure 5.12 — The BCAT2 shRNA sequence design.** The corresponding sense sequences are shown in red. The insert was ligated into a plasmid linearised by the restriction enzymes *Agel* and *EcoRI*. The sense and anti-sense sections are complementary and will anneal on transcription, with a hairpin loop forming at the *XhoI* sequence.

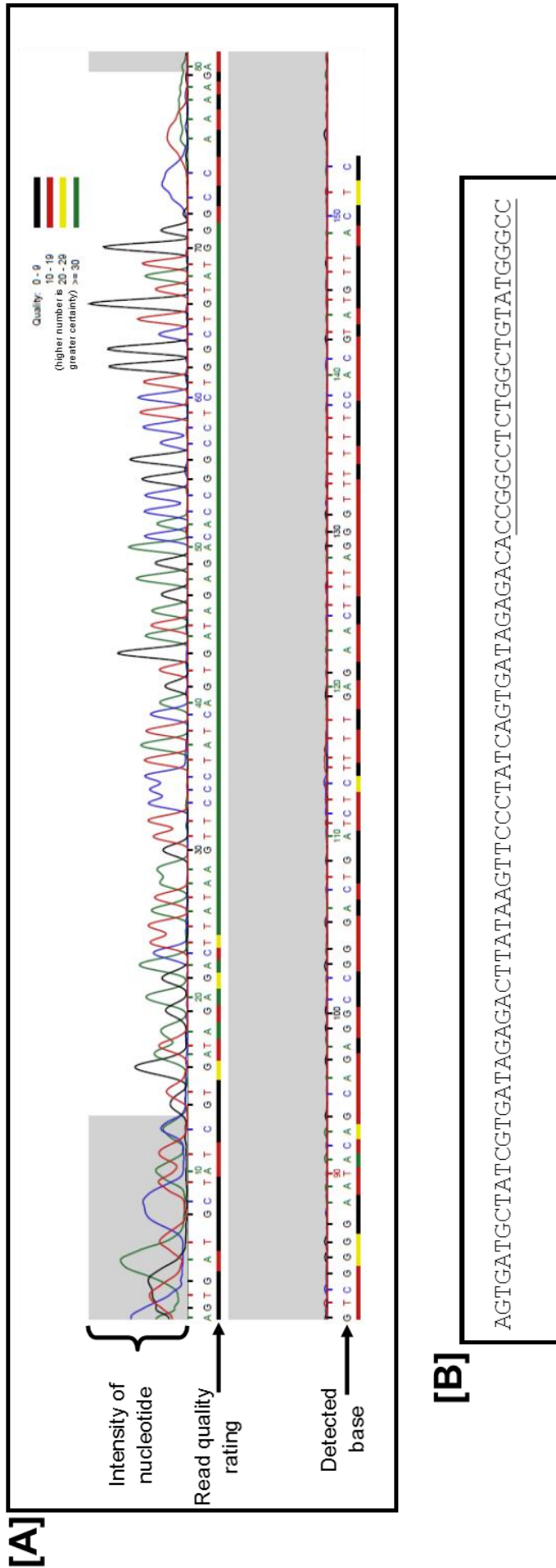


**Figure 5.13 — Partial sequence of pLKO-BCAT2 plasmid.** The plasmid was partially sequenced by an external laboratory (Eurofins MWG, Germany) using the pLKO1\_tet\_seq primer. **[A]** The quality report of the sequencing read appears to show a rapid termination of the sequencing progression, potentially due to the presence of an XhoI hairpin loop. **[B]** The bases which were correctly sequenced show homology to the shRNA sequence, which is marked by underlining.

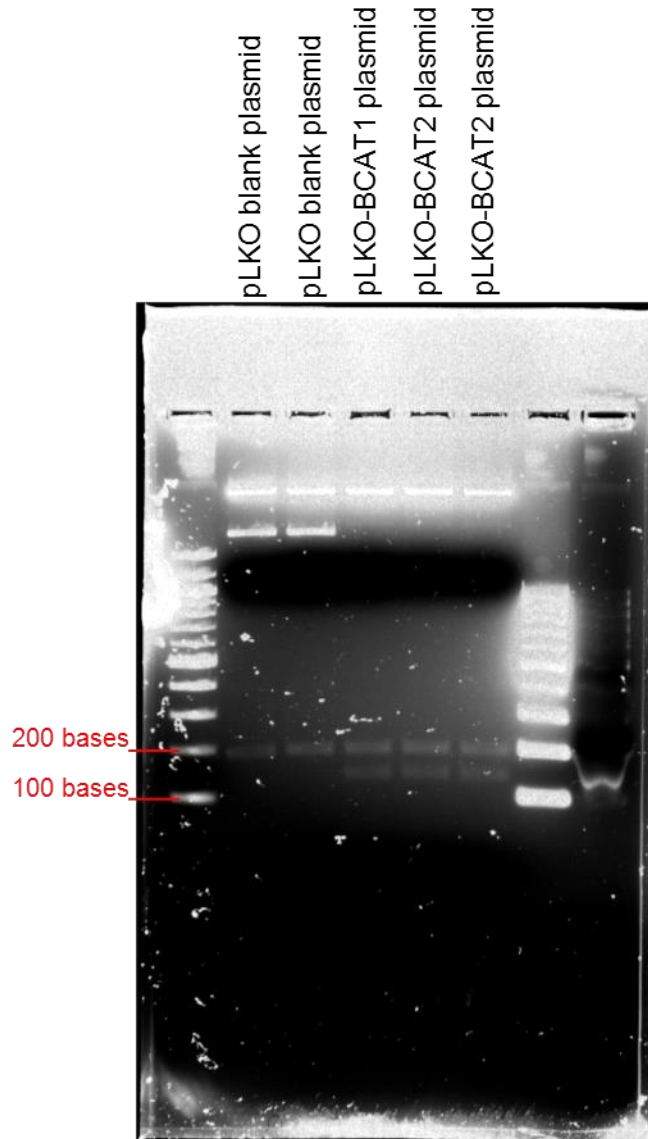


**Figure 5.14 — Digestion of pLKO-BCAT plasmids.** Plasmids were digested by incubation with the XhoI restriction enzyme. Individual 2% agarose gel lanes were loaded with different digested plasmid solutions or 100 base pair DNA ladder, and the gel electrophoresed. Once the run was complete the gel was stained with EthBr stain and imaged using a UV transilluminator. Upon digestion, a positive result for shRNA ligation is the presence of two bands of approximately 200 and 150 base pair length, while insertion ligation failure or the native unedited plasmid will only show one band of approximately 200 base pair length (Wiederschain *et al.*, 2009). Both the verified pLKO-BCAT1 and the new pLKO-BCAT2 plasmid show a double banding of approximately 150 and 200 base pairs, respectively.

## **5.4 – DISCUSSION.**

A main aim of this thesis was to develop a model of the human cerebrovasculature, which could be utilised to investigate the impact of hBCATm overexpression on BBB integrity, metabolomics, and redox status. It has been demonstrated here that a model was successfully constructed and permeability of the monolayer evaluated as a model of the BBB. In the first instance, rat astrocytes were used because of ease of accessibility, however, now that the method has been optimised this could be expanded to incorporate human astrocytes and also neurons. Furthermore, although there were difficulties in transfecting the hCMEC/D3 cell line, this was overcome by developing lentiviral plasmids as lentiviral transduction is effective in hCMEC/D3 cells (Mizee *et al.*, 2013).

### **5.4.1 – Validation of hCMEC/D3 monolayers as a representation of the BBB.**

To validate the culture model, hCMEC/D3 cells were first analysed by permeability studies. Monolayers were grown on collagen-coated transwell plate inserts and TEER measured using an EVOM meter and EndOhm chamber. Interestingly, this is not the only report of low TEER in hCMEC/D3 monolayers, and there appears to be a wide variation of findings in previous studies. For example, as previously described, Abbott *et al.* (2012) reported TEER values up to  $300 \Omega \times \text{cm}^2$ , while a detailed comparative study by Hatherell *et al.* (2011) found that co-culture with astrocytes produced monolayers with a TEER of  $63 \Omega \times \text{cm}^2$ . Conversely, Eigenmann *et al.* (2013) describe the cell line as unsuitable for studies using TEER due to low resistance, while the group whom developed and immortalised the cell line (Weksler *et al.*, 2005) also describe a low TEER value of  $< 40 \Omega \times \text{cm}^2$ . In these latter studies, the cell line was instead validated by demonstrating low monolayer permeability to radiolabelled or fluorescently labelled compounds (Weksler *et al.*, 2005).

In this thesis, the highest TEER observed was  $10 \Omega \times \text{cm}^2$ , therefore, the permeability of monolayers was instead assessed using the Na-Flu which is a fluorescent compound.

Permeability to this compound was examined over a period of 18 days and found to be within the previously reported range of  $3.4$  and  $5.5 \times 10^{-3} \text{ M cm}^{-1}$  (**Figure 5.3**) (Förster *et al.*, 2008). Further validation was carried out by western blot analysis for tight junction and adhesion proteins considered specific to brain microvascular tissue (Eigenmann *et al.*, 2013). It was determined that all three proteins investigated, VE-cadherin, occludin, and ZO-1, were expressed indicating that on the protein level, the cells were displaying the blood-brain barrier phenotype (**Figure 5.4**). Although two bands were observed on western blot analysis of VE-Cadherin of MW 89 and 115 kDa (**Figure 5.4; [A] [i]**), Vilgrain *et al.* (2013) were able to show definitively that the MW 115 kDa band is due to a glycosylation protein adduct and that western blot analysis of deglycosylated samples yields a single band of MW 89 kDa. In addition, western blot analysis of ZO-1 detected bands of a lower MW than expected (**Figure 5.4; [B] [i]**). Previously, western blot analysis of hCMEC/D3 cells found that the bands normally resolve at 220 kDa (Tai *et al.*, 2010) and it is therefore inconclusive as to whether ZO-1 is correctly detected in the cells. It has previously been demonstrated that the CaCO-2 epithelial cell line expresses ZO-1 protein (Anderson *et al.*, 1989; Wu *et al.*, 2014) and it is suggested here that western blot analysis could be used to compare ZO-1 expression in hCMEC/D3 cell and CaCO-2 cells. This could be used to troubleshoot the experiment as this could determine if the SDS-PAGE is not correctly resolving, if the antibody is not correctly detecting the protein detection, or if the protein is not expressed as expected in the hCMEC/D3 model. The next step in this thesis was the transfection of the endothelial cells with either RNAi or overexpression plasmids to modify the expression of hBCATm.

#### **5.4.2 – Transfection of the hCMEC/D3 cell line.**

Although transfection was easily achieved in SH-SY5Y cells, there was significant difficulty in transfection of the hCMEC/D3 cell line. The jetPRIME reagent was used in the first instance as it presented high rates of transfection in SH-SY5Y cells (**Figure 4.9**). Attempts were made to optimise the jetPRIME for use in hCMEC/D3 cells, however,

western blot analysis failed to detect any change in expression after transfection with either siRNA or expression plasmid (**Figure 5.5**). This was confirmed using fluorescent microscopy studies, whereby expression of eGFP (**Figure 5.6**) and internalisation of fluorescently labelled siRNA (**Figure 5.9**) was clearly inhibited in hCMEC/D3 cells.

There are currently no studies which describe plasmid transfection of hCMEC/D3 cells, although use of the RNAiMAX and DharmaFECT 1 siRNA transfection reagents has been described as effective in gene knock-down (Higuchi *et al.*, 2015; Jacob *et al.*, 2015; Hurst *et al.*, 2012). Using RNAiMAX it was found that a 12.5 nM siRNA transfection reduced hBCATm expression 85% in hCMEC/D3 cells (**Figure 5.10**). Interestingly, lower concentrations of siRNA appeared to decrease expression the most, and further work could determine if lowering siRNA concentration further would improve the efficiency of knock-down. As there is no published data on the transient transfection of plasmids into the hCMEC/D3 cell line and it was not possible in this study, it is considered that this cell line is not suitable for transient transfection. It was therefore decided to design lentiviral vectors for the stable transduction of doxocycline-inducible shRNA and mRNA expression.

#### **5.4.3 – Development of lentiviral vectors for stable inducible transfection.**

Transduction with a lentiviral vector is well characterised as a highly efficient method capable of transducing several transfection resistant cell types (Blömer *et al.*, 1997; Dull *et al.*, 1998). For example, lentiviral vectors are capable of transducing post-mitotic cells with a near 100% efficiency (Naldini *et al.*, 1996), while other methods such as calcium-phosphate-DNA co-precipitation, electroporation, and cationic lipid transfection typically have transfection efficiencies of < 25% and in many cases are completely ineffective (Ohkia *et al.*, 2001). In particular, lentiviral transduction has been described as capable of generating genetically modified hCMEC/D3 cells (Mizee *et al.*, 2013). The vectors could also be used to transduce the SH-SY5Y cells to remove the need for transient

transfection and create a stable cell line with transcription activated by treatment with tetracycline or doxycycline (Wiederschain *et al.*, 2009).

Both of the shRNA sequences were inserted into the tet-pLKO-puro plasmid. This plasmid was selected because of the well-designed inducible expression system (Wiederschain *et al.*, 2009). The BCAT1 shRNA vector was kindly provided by Dr Bernhard Radlwimmer (DKFZ German Cancer Consortium, Germany) (Tönjes *et al.*, 2013), while the BCAT2 shRNA was designed based on the already validated siRNA sequence from this study. The BCAT2 siRNA begins with 'AA' nucleotide bases as the sequence; however, the shRNA begins 'CC' nucleotide bases, as this was used by the group whom designed and tested the tet-pLKO-puro plasmid (Wiederschain *et al.*, 2009). Annealing of the shRNA sequence was confirmed with a diagnostic digest (**Figure 5.11**). Attempts to sequence the BCAT2 shRNA were only partially successful as the sequencing process stopped abruptly at the point of the hairpin loop, suggesting that the sequencing enzyme could not bind to the loop. However, the manufacturer's instructions for tet-pLKO-puro shRNA synthesis only propose the diagnostic digest and this, along with the partial sequence, is considered sufficient.

Likewise, the two hBCAT expression plasmids were synthesised by cloning the respective cDNA sequence into the pCW57.1 lentiviral plasmid using the gateway recombination system. The hBCAT expression plasmids were generated by a recombination event between the entry clone (containing the hBCAT gene) and the destination vector (containing the TetR promoter), before transformation into *E. coli*. Additionally, the BCAT2 gene in the entry clone was codon optimised by the manufacturer (Fisher Scientific, Loughborough) to improve protein expression in human cells. This was conducted by modifying the base sequence so that the same protein was produced from the same amino acid sequence, but the codons used were the most abundant in the host species, with the aim of increasing protein yield (Kim *et al.*, 1997). Correct synthesis of the expression plasmid was confirmed by partial sequencing

**(Appendix B; 2).** Expression of the respective isoform can again be induced by treatment of transduced cells with an appropriate concentration of tetracycline or doxycycline. The plasmid has been successfully used by other groups for pteoin expression (Momocilovic *et al.*, 2015; Barger *et al.*, 2015). All of the required lentiviral plasmids were synthesised and transformed into *E. coli* for long term storage, although unfortunately time constraints determined that lentiviral particle generation and mammalian cell transduction was not possible. However, due to the current work, all of the required materials are in place for future experimentation and development.

#### **5.4.4 – Summary.**

An *in vitro* human brain model is required to replace animal models due to the unique expression of hBCATm in the human brain. The first step in this is the modelling of the BBB. In this thesis, a BBB model was constructed which expresses the expected TJ proteins and has a membrane permeability similar to previous studies (Förster *et al.*, 2008). This model can be utilised for future studies into the impact of hBCAT and BCAA metabolism on BBB integrity and permeability. Unfortunately, the endothelial cells of the culture appeared to be resistant to transfection. Knock-down of hBCATm was not achieved until the end of the project and it was not possible to investigate the impact of this. Furthermore, overexpression of protein was not achieved under a variety of conditions, although there are no published examples of plasmid transfection in this cell line, suggesting that it may not be currently achievable. To circumvent this, lentiviral plasmids for viral transduction were designed and synthesised for future work.